Dyes and Pigments 92 (2011) 758–765

Contents lists available at ScienceDirect

Dyes and Pigments

journal homepage: www.elsevier.com/locate/dyepig

Study on the interaction of Basic Violet 2 with hydroxypropyl-β-cyclodextrin

Ivana M. Aiassa Martínez [a], María N. Montes de Oca [b], Ana G. Iriarte [a], Cristina S. Ortiz [b], Gerardo A. Argüello [a,*]

[a] INFIQC – Dpto. de Fisicoquímica, Universidad Nacional de Córdoba, Ciudad Universitaria, 5000 Córdoba, Argentina
[b] Dpto. de Farmacia, Facultad de Ciencias Químicas, Universidad Nacional de Córdoba, Ciudad Universitaria, 5000 Córdoba, Argentina

ARTICLE INFO

Article history:
Received 29 December 2010
Received in revised form
8 June 2011
Accepted 20 June 2011
Available online 12 July 2011

Keywords:
Triarylmethanes
Basic Violet 2
Cyclodextrin
Photosensitizer
Association constant
Visible spectroscopy

ABSTRACT

The formation of the inclusion complexes of Basic Violet 2 (New Fuchsin) with hydroxypropyl-β-cyclodextrin (HP-β-CD) was studied by UV–Vis absorption and fluorescence spectroscopy. The binding constants of the inclusion complexes, K_B, were obtained considering the maximum shift of the absorption spectra, the absorption areas deconvoluted as the sum of two gaussian constituents, the relative fluorescence quantum yield and the fluorescence maximum shift. The values achieved were $2.7 \times 10^3\ M^{-1}$, $0.95 \times 10^3\ M^{-1}$ and $2.8 \times 10^3\ M^{-1}$, $2.2 \times 10^3\ M^{-1}$, respectively. *Ab-initio* calculations using B3LYP/6-31G level of approach and the natural bond orbital (NBO) analysis were performed to gain a deeper understanding of the inclusion phenomena. The result showed a high complexation in aqueous media.

1. Introduction

Photodynamic therapy (PDT) is a treatment modality, which has demonstrated the ability to detect and eradicate cancer. The PDT acts through at least three principal mechanisms: direct cell killing by lethal oxidative damage to tumor cells; indirect cell killing due to photodynamic damage to, or shutdown of, the (neo)vasculature with loss of oxygen and nutrients to the tumor; and additional anti-tumor contributions from the inflammatory and immune responses of the host. The three components are deemed necessary for the best long-term response; however, their relative roles vary considerably depending on the photosensitizer, its subcellular and tissue distribution, the tumor type and its microvasculature, and the type and duration of inflammatory and immune responses elicited in the host [1]. This therapy uses light activated drugs, with an appropriate wavelength, to trigger a photochemotherapeutic mechanism capable of destroying tumor cells selectively. The preferential localization of the drug allows a selective activation, thereby causing a cytotoxic reaction at lethal levels in dysplastic lesions and fully developed carcinomas [2–4].

As discussed in Allison et al. clinically relevant photosensitizers can be classified into one of three broad chemical families: (i) porphyrins, formed in most cell types from their precursor δ-aminolevulinic acid (ALA); (ii) chlorophyll derivatives; and (iii) dye substances. Second-generation photosensitizers are pure in a chemical sense and offer high quantum yields for the triplet state generation and formation of reactive oxygen species (ROS) [5]. The study of cationic dyes, in particular triarylmethanes (TAMs) and their derivatives, is increasingly being conducted in medicine due to their potential use as photosensitizing agents. The electrical potential across the mitochondrial membrane in tumor cell is much more negative (around 60 mV) than that in normal cells [6]. It is believed that this fact is responsible for a preferential accumulation of the dye bearing the localized positive charge in tumor cells. Thus, the photosensitizer (dye) combined with light at mitochondrial level should promote the neoplasic cell death.

The selective phototoxicity of some TAMs towards tumor cells indicates that these dyes display structural features that could be used as guidelines for the development of new techniques to treat neoplasic diseases [7]. Furthermore, TAM dyes have been reported to be active against intestinal helminths, filariae, trichomonads and trypanosomes [8]. In current clinical practice, PDT is considered an ablative procedure directed mainly at oncologic target and their vascular supply [9].

Research on molecular recognition has attracted much attention in supramolecular chemistry involving host-guest system to be used especially as drug carrier to reach specific targets. Cyclodextrins (CD) are commonly used to study those systems which consist

* Corresponding author. Tel.: +54 351 4334180; fax: +54 351 4334188.
E-mail address: gerardoa@fcq.unc.edu.ar (G.A. Argüello).

0143-7208/$ – see front matter © 2011 Elsevier Ltd. All rights reserved.
doi:10.1016/j.dyepig.2011.06.027

of six (α-CD), seven (β-CD) and eight (γ-CD) sugar units. CDs are generally represented as truncated cones with conical cavities capable of incorporating selectively a great variety of organic guests to form inclusion complexes in aqueous solutions. The cavity within CDs is hydrophobic and less polar than the surrounding water molecules. The complexation phenomenon often results in a significant variation in the photophysical and photochemical properties of guest molecules due to the microenvironmental difference inside the CD and the aqueous medium [10]. A correct interpretation of the inclusion phenomenon and an accurate determination of the binding constants of these complexes are fundamental topics to such investigations. Current methods for the measurement of the inclusion constant include UV–Vis spectrophotometry, spectrofluorometry, as well as electrochemical methods.

A wide variety of studies of TAMs have been previously reported, including their use in photodynamic antimicrobial chemotherapy [11,12], protein binding [13–15] and their behavior in different solvents [16,17], among others [18–20]. Nevertheless, although Basic Violet 2 (New Fuchsin, see Scheme 1) belongs to the TAM family, only scarce information on this dye can be found in the literature. Its absorption spectrum in solution appears to be composed of two bands which have been interpreted on the basis of the existence of two ground states in equilibrium [21–25]. It was also proposed that one of these bands should correspond to a propeller structure (D_3 symmetry), already identified as a ground-state structure of Basic Violet 3 (Crystal Violet) [26–28]. The other band should correspond to the distorted propeller arrangement caused by the rotation of two phenyl rings and the third phenyl ring having a double bond with the central carbon, in which the positive charge is located on the amine group of the last phenyl group (C_2 symmetry). This structure is expected by the molecular arrangement of Basic Violet 3, although no evidence for could be found for C_2 isomer, some studies arguing against this structure [21–25,29–31].

In a particularly interesting study concerning Basic Violet 3 and using different alcohols as solvents, Maruyama et al. suggest the presence of two ground-state isomers in equilibrium; one of these is a planar ground-state structure of Basic Violet 3 having D_3 symmetry; the other with the three bonds on the central carbon bent out of plane having a pyramidal structure with C_3 symmetry. The isomerization rate is reported to be independent of the solvent viscosity (rate of about 500 fs for several alcohols) [25,32]. For example, Basic Violet 2 could have two or more solvatation forms interacting with polar solvent molecules. When the solvent molecule approaches the central carbon, it would be pulled outside, thus the planar (D_3) structure of Basic Violet 2 may become pyramidal (C_3). When the interaction between the central carbon and the solvent molecule breaks, Basic Violet 2 returns to the propeller structure. Since Basic Violet 2 solvated with a solvent molecule close to the central carbon should have a rather lower energy, the pyramidal structure (C_3) should correspond to the isomer of lower energy (maximum of the absorption band), and the propeller structure (D_3) to the isomer of higher energy (shoulder of the absorption band).

In this paper, we report the experimental results of UV–Vis absorption and fluorescence emission spectra studies of the inclusion complexes between Basic Violet 2 and hydroxypropyl-β-cyclodextrin (HP-β-CD). The absorption spectra were examined by a theoretical treatment, taking into account the absorption bands (from 400 nm to 650 nm) resolved as the sum of two gaussian constituents, and in accordance with the existence of the two isomers, namely D_3 and C_2. *Ab-initio* calculations, using B3LYP/6-31G level of approach; natural bond orbital (NBO) analyses were performed to understand both the inclusion phenomena and the implication that the dye symmetry has over the inclusion complex's spectroscopic behavior.

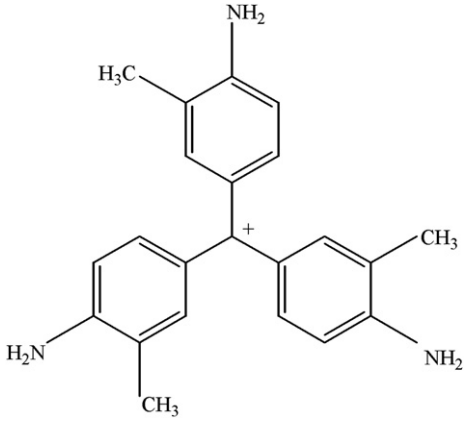

Scheme 1. Basic Violet 2 molecule.

2. Experimental

2.1. Materials

The commercial product Basic Violet 2 (Scheme 1) was obtained from Sigma Chemical Co. (St. Louis, MO) and purified chromatographically. A silica gel (70–230 mesh, Sigma Chemical Co.) filling a 750 mn × 23 mm glass tube was used as the preparative column, and the purity was confirmed by HPLC in a Waters Spherisorb ODS 2; 250 × 4.6 mm, 5 μm (Supelco Inc) [33].

HP-β-CD was kindly supplied by Cerestar USA, Inc Lot G 8120. D-(+)-Glucose was obtained from Sigma. Milli-Q grade water was used. 2-Propanol (Sintogran HPLC grade) was used without further purification. All other chemicals were analytical grade.

2.2. Methods

Absorption spectra were recorded using an Agilent 8453 UV–Vis spectrophotometer with diode array detector and 1 nm resolution. Steady-state luminescence measurements were performed using a Quanta Master QM2 Spectrofluorometer from PTI (Photon Technology International) equipped with a Hamamatsu R928 PMT in a photon counting detector. The samples were excited at λ_{exc} = 500 nm and the corrected fluorescence spectra were acquired from 520 to 800 nm. The relative fluorescence quantum yield of NF was taken as the ratio between the area under the fluorescence spectrum at different CD concentrations and the fluorescence spectrum in the absence of CD.

In a typical experiment the solutions were prepared one day before and maintained in the refrigerator; the concentrations of Basic Violet 2 were kept on $\sim 1.00 \times 10^{-5}$ M and [HP-β-CD] varied from 0 to 8.24×10^{-3} M. The experiments were carried out at room temperature in aqueous solutions. The possible formation of Basic Violet 2 aggregates in aqueous solution was previously tested. The absorption spectra of the dye at different concentrations ranging from 0.64 to 2.2×10^{-5} M were recorded. The normalized spectra at 546 nm did not show significant changes in its shape (data not shown), which allowed concluding that, in this concentration range, Basic Violet 2 did not form aggregates.

Origin 7.0 of OriginLab Corporation software was used to evaluate the association constants by linear least square fitting. The fitting process was achieved in agreement with Benesi-Hilderbrand

1:1 equilibrium and the deconvolution according to two gaussian components of the absorption bands [34].

2.3. Computational details

In order to perform the potential energy surface study, the Basic Violet 2-β-CD system was chosen for the analysis due that it was describe in the literature a very good concordance in the inclusion of a guest with HP-β-CD or α-CD as host [35,36]. This selection has also considered that this system represents a less-consuming calculation time. With this in mind, geometrical parameters were obtained by *ab-initio* calculations, using B3LYP method [37–39]. The Basic Violet 2, β-cyclodextrin (β-CD), and Basic Violet 2-β-CD complex geometries were optimized using standard convergence criteria without symmetry restrictions. Frequencies were evaluated to check that the calculated geometry corresponded to a minimum in the potential energy surface, and to assess the zero-point energy. The 6-31G basis set was used with the B3LYP method. All calculations were performed with the Gaussian 03 Package [40]. The NBO analysis was carried out using the 3.1 version of the NBO package included in the program, with a higher level of basis set (6-311 + g**) [41,42].

3. Results and discussion

3.1. Formation of the inclusion complexes of Basic Violet 2 with cyclodextrin

Absorption and emission spectra of Basic Violet 2 were taken in the presence and absence of different HP-β-CD concentrations and the effect on the absorption and emission intensities was observed. Interestingly, the results show that both spectra depend on the concentration of HP-β-CD. The maximum absorption wavelength of pure Basic Violet 2 lies on 546 nm. When an increasing concentration of HP-β-CD occurred, the absorbance at the maximum gradually decreased in the range of low HP-β-CD concentrations reaching a minimum; it then increased in the range of high concentrations. In any case, a shift to longer wavelength (from 546 to 558 nm) was observed in the absorption spectrum. It can also be observed that the shoulder becomes less pronounced when increasing [HP-β-CD] (further discussed below). The emission spectrum also showed the same shift effect although less pronounced. Fig. 1 depicts the experimental results.

The photophysical and photochemical properties of the guest molecule are altered due to the formation of a host–guest complex (Basic Violet 2-HP-β-CD). To understand the changes found in the absorption and emission spectra of the Basic Violet 2 in the presence of HP-β-CD, different contributions to the global changes must be taken into account.

In order to distinguish the spectra modification produced by the inclusion of the dye in the CD cavity from other effects (nonspecific interaction between dye and CD or changes in solvent properties due to the presence of CD) and to confirm the formation of the complex, two tests were performed: the glucose and the alcoholic test. Absorption and emission experiments were carried out using D-(+)-glucose and different 2-propanol:water mixtures instead of HP-β-CD to study solvent effect and changes in the polarity (to mimic the hydrophobic environments) respectively, when dye is included in the cavity.

3.1.1. Glucose test

Amounts of D-(+)-glucose (monomer of CD) comparable to those of the CD were used. The effect of glucose solutions was tested, like a solvent, on absorption and emission spectra, knowing that the inclusion effect was not possible. Fig. 2 shows that when

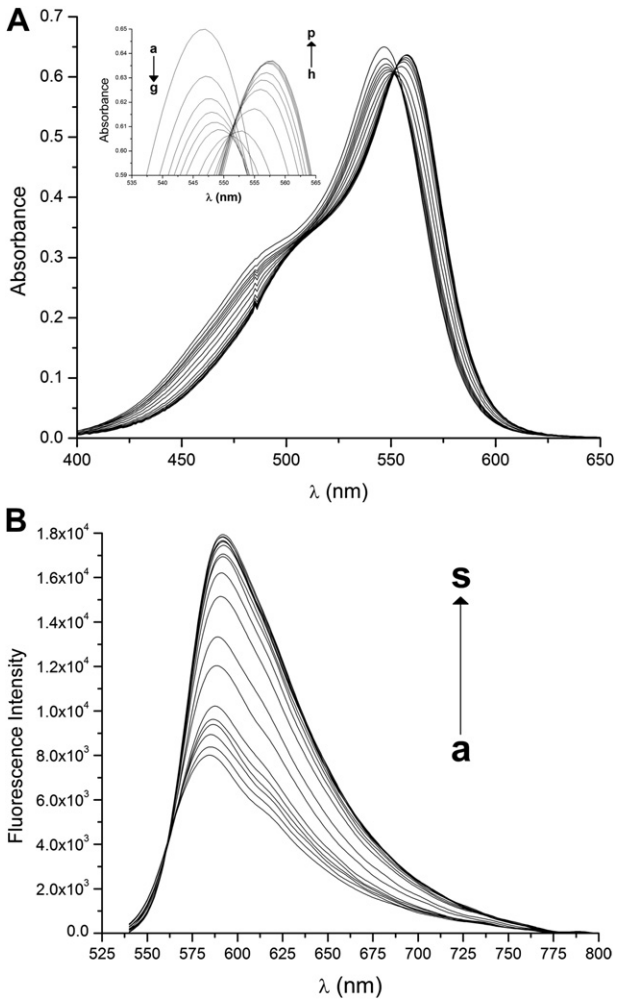

Fig. 1. A. Basic Violet 2 absorption spectrum in the presence of different concentrations of HP-β-CD. From left to right, the HP-β-CD concentration varied from 0 to 6.18×10^{-3} M. B: Fluorescence spectra of Basic Violet 2 in the presence and absence of HP-β-CD (0–$8.24\ 10^{-3}$ M) in water. All concentrations (a to s) are detailed in Table 1.

the glucose concentration increases, the absorption maximum at 546 nm gradually decreases in the range of the concentration studied without causing changes in the position of λ_{max}. On the other hand, the fluorescence quantum yield decreases when glucose is added in the range of low concentration. However, by increasing the glucose concentration, the quantum yield reaches a minimum and rises slowly, and no λ_{em} shift was found either. The decrease in the quantum yield at low concentrations is consistent with the variation found in the absorption spectrum, and at high glucose concentrations, the slight increase observed in the quantum yield could be attributed to changes in viscosity and/or a specific interaction between glucose and Basic Violet 2. Taking into account that no shift, λ_{max} or λ_{em}, was observed, the results differed from those found when CD was added, confirming that the CD induces other spectral changes that could be attributed to the formation of an inclusion complex.

3.1.2. Alcoholic test

The polarity of the hydrophobic cavity of CDs is similar to that of the alcohols (i.e., 2-propanol). In order to test whether the inclusion derives from changes in the polarity of the medium, the absorption and emission spectra of Basic Violet 2 were investigated at different 2-propanol:water percentages from 0:100 to 100:0 (Fig. 3). It can be

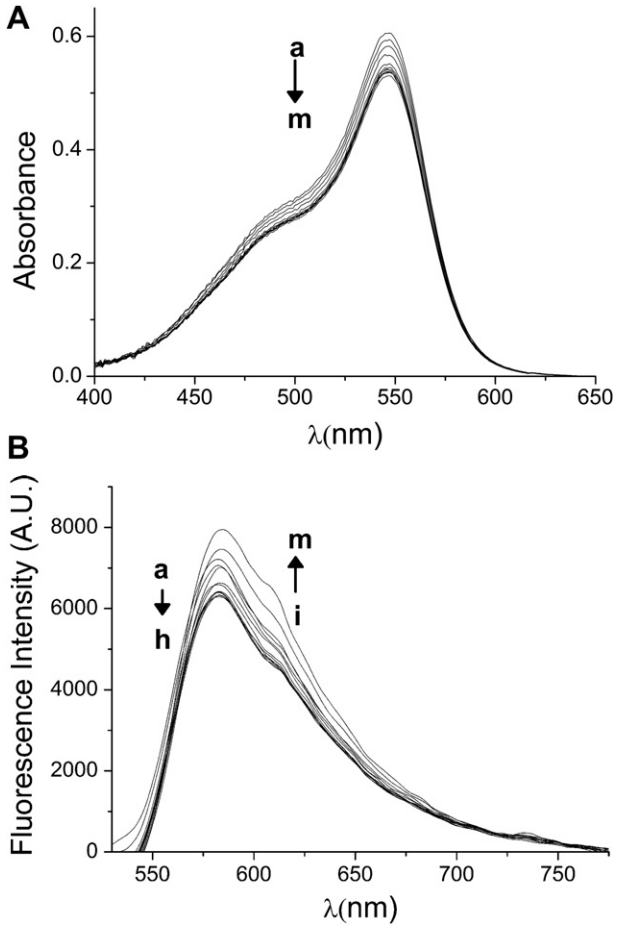

Fig. 2. Absorption and emission spectra of Basic Violet 2 in the presence of various concentrations of glucose. The glucose concentrations used were a = 0; b = 2.63×10^{-6}; c = 1.01×10^{-5}; d = 2.04×10^{-5}; e = 4.04×10^{-5}; f = 7.90×10^{-5}; g = 1.58×10^{-4}; h = 3.13×10^{-4}; i = 6.45×10^{-4}; j = 1.31×10^{-3}; k = 2.50×10^{-3}; l = 5.06×10^{-3}; and m = 6.71×10^{-3} M.

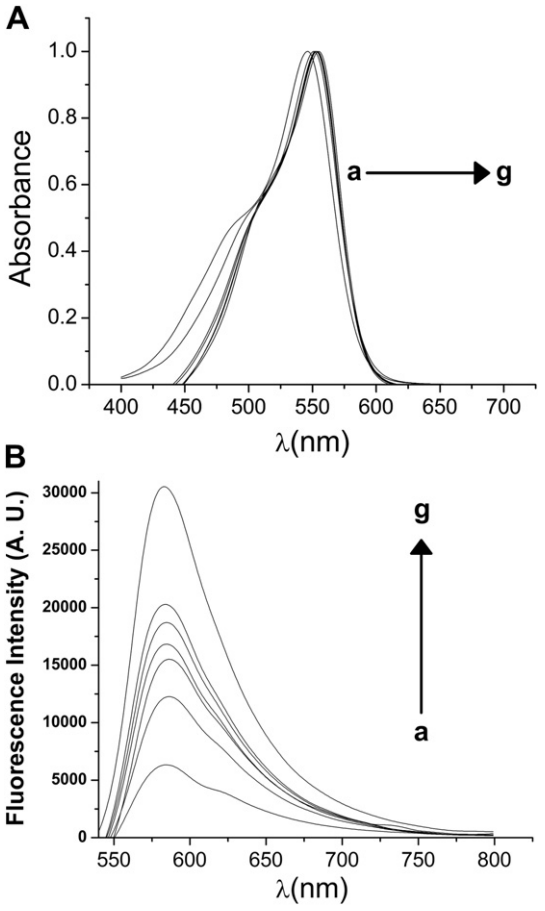

Fig. 3. Absorption and emission spectra of Basic Violet 2 in the presence of various percentages of 2-propanol. For the fluorescence graph (from bottom to top), and for the absorbance graph (from left to right), the 2-propanol:water relation was a = 0:100, b = 20:80, c = 40:60, d = 50:50, f = 60:40, g = 80:20, h = 100:0.

seen that the absorption spectrum does not change its shape and shows a batochromic shift from 546 to 555 while the 2-propanol percentage increases. As the percentage of 2-propanol in the mixed solvents increases, the fluorescence intensity is considerably enhanced with no significant λ_{em} shift.

In view of the results described, the changes observed in Fig. 1A can be interpreted as revealing a combined effect of the CD as a solvent (decrease in the absorption bands) and the inclusion effect (increase in the absorption band with the batochromic shift). The enhancement of the emission intensity at high concentrations of CD can be attributed to the inclusion effect (Fig. 1B); this suggests that, due to the steric restriction imposed by the CD cavity on the rotation of amine ring of Basic Violet 2, a fluorescence quantum yield is larger than that of the free dye in solution.

3.2. Determination of association constants

The formation of a complex between Basic Violet 2 and HP-β-CD can be represented as:

$$dye + CD \rightleftarrows dye \cdot CD \quad (1)$$

where *dye* stands for *Basic Violet 2* and *dye·CD* denotes the association complex, which may be a surface or an inclusion complex in aqueous or non-aqueous media. The expression for the binding constant is given by:

$$K_B = \frac{[dye \cdot CD]}{[dye][CD]} \quad (2)$$

The formation constant for the binary complex between CD and Basic Violet 2 can be evaluated using the Benesi–Hildebrand equation (3):

$$\frac{1}{\lambda - \lambda_0} = \frac{1}{K_B \times (\lambda_{CD} - \lambda_0) \times [CD]_0} + \frac{1}{\lambda_{CD} - \lambda_0} \quad (3)$$

where λ, λ_o and λ_{CD} represent the wavelength of the maximum absorption as function of HP-β-CD concentration, the wavelength of the maximum absorption without HP-β-CD, and the wavelength of the maximum absorption when a large amount of HP-β-CD is added, respectively [43]. This equation can be used whenever the [HP-β-CD] >> [Basic Violet 2] condition is fulfilled. In our case, this last condition holds since the [HP-β-CD]/[Basic Violet 2] ratio in concentrations is larger than 10^3. Fig. 4 shows Benesi–Hildebrand plot for a 1:1 equilibrium according to Eq. (3) and least square linear fit analysis, yielding a value of K_B equal to $(2.7 \pm 0.2) \times 10^3$ M^{-1}. This value is good agreement with the data cited in the literature for similar systems considering a 1:1 host–guest equilibrium [32,44,45]. In addition, it is necessary to indicate that the results obtained were not coherent when the fitting process was achieved in agreement with Benesi–Hilderbrand 1:2 equilibrium and the

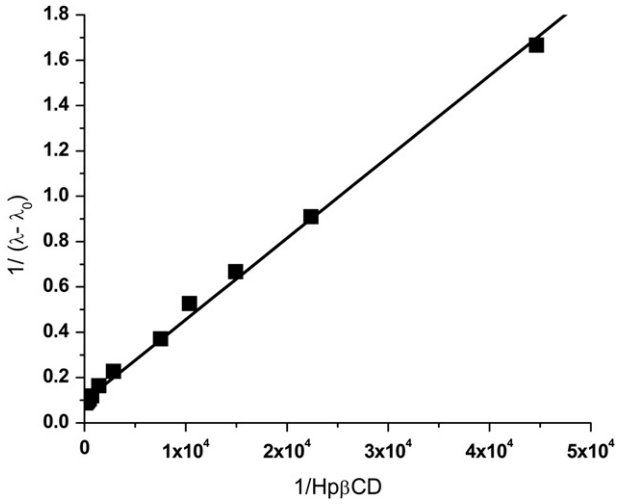

Fig. 4. Benesi-Hildebrand for the shifting of λ_{max} as a function of [HP-β-CD]; the concentration of Basic Violet 2 was 1.00×10^{-5} M and [HP-β-CD] was varied from 0 to 8.24×10^{-3} M.

Table 1
Percentage of the theoretical areas for the Gaussian components calculated from the deconvolution of the absorption spectra at different HP-β-CD concentrations.

Nomenclature	[HP-β-CD] M	% A_1 (*G1*)	λ_1 (nm)	% A_2 (*G2*)	λ_2 (nm)	λ_{total} (nm)	$\Delta\lambda$ (nm)
a	0	65.0	506	35.0	549	546	43
b	2.24×10^{-5}	65.0	506	35.0	550	547	44
c	4.47×10^{-5}	64.8	507	35.2	550	547	43
d	6.69×10^{-5}	65.0	508	35.0	551	547	43
e	9.64×10^{-5}	64.9	509	35.1	551	548	42
f	1.33×10^{-4}	64.7	509	35.3	552	549	43
g	3.48×10^{-4}	65.4	512	34.6	554	550	42
h	7.01×10^{-4}	66.1	514	33.9	555	552	41
i	1.38×10^{-3}	67.4	517	32.6	557	554	40
j	2.07×10^{-3}	68.1	519	31.9	558	555	39
k	2.76×10^{-3}	68.4	520	31.6	559	555	39
l	3.39×10^{-3}	68.8	521	31.2	559	556	38
m	4.12×10^{-3}	69.0	521	31.0	559	556	38
n	4.79×10^{-3}	69.1	522	30.9	559	556	38
o	5.45×10^{-3}	69.2	522	30.8	560	557	38
p	6.18×10^{-3}	69.1	522	30.9	560	557	38
q	6.86×10^{-3}	69.3	522	30.7	560	557	38
r	7.53×10^{-3}	69.4	522	30.6	560	557	38
s	8.24×10^{-3}	69.4	522	30.6	560	557	38

deconvolution according to three gaussian components of the absorption bands.

As we stated above, Fig. 1 shows that the shoulder becomes less pronounced when increasing [HP-β-CD]. The absorption spectra were analyzed theoretically as composing of several gaussian curves. The deconvolution was done using two and three components and the best results were achieved with two gaussians. The fitting process was carried out using Eq. (4), where *A*, *w* and λ stand for the absorption intensity, the width and the maximum wavelength for the individual gaussian corresponding to the shoulder (s) and the maximum (m), respectively.

$$y = y_0 + \frac{A_s}{w_s\sqrt{\pi/2}} e^{-2\left(\frac{\lambda-\lambda_s}{w_s}\right)^2} + \frac{A_m}{w_m\sqrt{\pi/2}} e^{-2\left(\frac{\lambda-\lambda_m}{w_m}\right)^2} \quad (4)$$

According to the theoretical data we propose the existence of two isomers in equilibrium (D_3 and C_2, see below). In the absence of HP-β-CD, the highest energy gaussian component is centered at $\lambda_s = 506$ nm (shoulder) and should correspond to the C_2 isomer of the ground state while the gaussian with lowest energy $\lambda_m = 549$ nm (maximum) should correspond to the D_3 isomer. The last one gains relevance when the dye is included in the HP-β-CDs. Table 1 shows the parameters obtained from the fitting process. By increasing [HP-β-CD], a slight decrease in $\Delta\lambda(\Delta\lambda = \lambda_m - \lambda_s)$ is observed and it could be interpreted as a Basic Violet 2 migration to a less polar medium (from aqueous medium to a less polar CD cavity) [46]. These results confirm that the formation of complexes promoted by an increase in the HP-β-CD concentration produces a shift in the host–guess equilibrium 2 with both gaussian parameters (λ_m and λ_s) showing a bathochromic effect. As seen from Eq. (4), the percentage of the area of the first gaussian (*G1*) in the absence of the HP-β-CD is 65.0%; however, when [HP-β-CD] increases up to 8.24×10^{-3} M, this area shows a steady increase up to 69.4%. In view of the change in the theoretical percentage of the gaussian areas and using eq. (3), the binding constant was estimated in $K_B = (0.95 \pm 0.05) \times 10^3$ M^{-1}, correlating closely with the experimental absorbance value (Fig. 5). The model for representing the absorption spectra of TAMs considering as composing of a series of additive gaussian functions was successfully applied in several studies [25,32,47,48]. The aim of this analysis was to evaluate the model by comparison with the association constants obtained experimentally by absorption and fluorescence. In the present study, a good fitting was achieved considering the absorption spectrum as the sum of only two gaussian functions. The theoretical association constant calculated taking into account the areas of its component gaussians correlates quite well with the experimental results, allowing us to corroborate the validity to the model used.

The binding constant was also calculated from the relative quantum yield and fluorescence maxima shift data from the emission spectrum using also Eq. (3). Due to the low fluorescence quantum yield of this system, the experimental data show error larger than that of the absorption data.

Table 2 shows K_B values for the different alternatives of calculation. The values of the calculated constants confirm the formation process of complex; in all cases similar values were also obtained with good correlation coefficients. Further, the constant calculated by the theoretical areas correlated very well with those from experimental data and in all cases the results indicated a 1:1 stoichiometry.

3.3. Ab-initio calculus

Theoretical calculations (geometry optimizations, frequencies and electronic delocalizations) were performed to gain further insight into interactions between Basic Violet 2 and β-CD. In order to represent adequately what was experimentally observed, calculi in water as solvent (using the PCM model) and with 6-311G bases set were attempted to perform. However, it was computationally highly expensive, and the convergence criteria could not be reached. For this reason, all the calculations were carried out considering the systems at vacuum and at 6-31G level of approach. For the sake of simplicity, Basic Violet 2 and β-CD have been chosen on the grounds that the latter provides the same information on the inclusion phenomenon, as mentioned before.

The structure of β-CD in solution, obtained by ONIOM2 method [49] was reported. These results show a β-CD molecule slightly distorted on the tip of the truncated cone, due to the deviation of some of the OH- groups in water. The energies of the distorted and not-distorted β-CD and the Basic Violet 2 molecules were calculated to obtain the stabilization energy originated by the formation of the inclusion complex in both systems (Basic Violet 2-β-$CD_{distorted}$ and Basic Violet 2-β-$CD_{not\text{-}distorted}$).

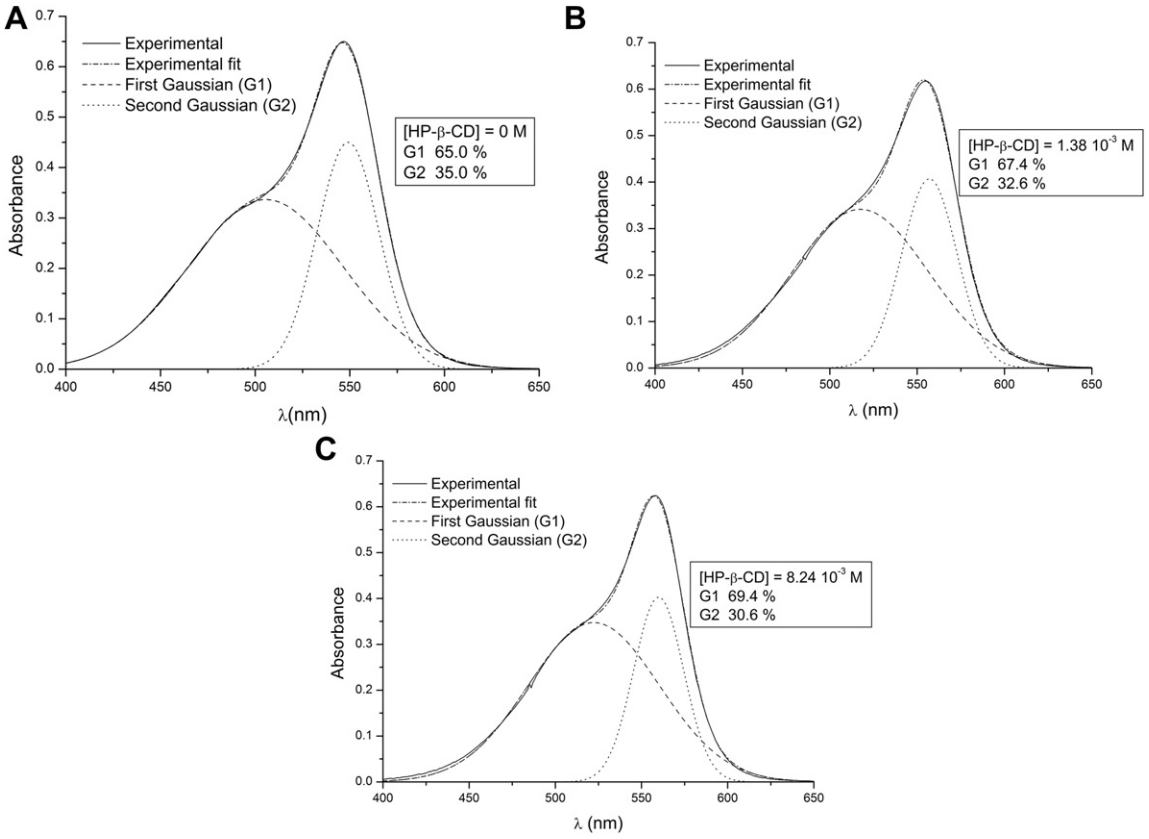

Fig. 5. Deconvolution of the Basic Violet 2 absorption spectrum in the corresponding Gaussian components at different HP-β-CD concentrations. The concentration of Basic Violet 2 was 1.00×10^{-5} M and [HP-β-CD] = a) 0.0 M; b) 1.38×10^{-3} M; and c) 8.24×10^{-3} M.

The NBO analysis was performed in order to make a deeper study of the magnitude of the electronic interactions between the Basic Violet 2 and the β-CD molecules.

3.3.1. Conformational analysis

As mentioned in 3.3 section, β-CD presents a distortion in aqueous media according to the theoretical calculations. As all the calculus must be carried out in gas phase, we have considered both structures as possible in the complex formation. The lower complex energy interaction corresponds to the Basic Violet 2-β-$CD_{distorted}$ system, which is also about 43.54 Kcal mol^{-1} more stable than the energies of each compound at vacuum. This energy value (lower than that of a net bond) is large enough to account for the complex stability in comparison with the isolated species. Thus, hereinafter, the β-CD and Basic Violet 2-β-CD systems shall be referred to as systems with β-$CD_{distorted}$.

A notable aspect to take account of is the change in the symmetry of Basic Violet 2, from D_3 (free species) to C_2 symmetry (complexed species). This fact is in agreement with our spectroscopic results. In a top view of the Basic Violet 2-β-$CD_{distorted}$ system, it was possible to note that the almost double bond character of the C—C bond around the central carbon atom was approximately 0.07 Å shorter than the average of the other two C—C bonds. This fact could be associated with the electronic delocalization arisen when the dye interacts with the β-CD, changing their symmetry.

Taking into account the β-CD, conformational changes in the seven hydroxyl groups placed on the base of the β-CD were observed as a result of their interaction with the dye. Fig. 6 shows the main points of interaction. After the introduction of the Basic Violet 2 inside the β-CD, one of the hydroxyl groups rotates and points outwards with respect to the β-CD ring (Fig. 6A). This conformation allows the interaction between one of the remaining six hydroxyls (that lies at the bottom), and the amine group inside the cavity via hydrogen bond. A more clear explanation could be obtained from the NBO analysis. Table 3 shows the most relevant electronic delocalizations for both systems (distorted and not-distorted complexes). According to the NBO, the closer dye-β-CD interaction takes place when the cyclodextrin has a distorted form. For the latter case, the higher stabilization energy (16.93 Kcal mol^{-1}) is given for the electronic delocalization from one of the oxygen lone-pair orbital of the β-CD to the σ nitrogen-hydrogen antibonding orbital of the Basic Violet 2 (denoted as $Lp(2)\ O_{77} \rightarrow \sigma^{*}N_{170}{-}H_{171}$); this interaction is not observed in the not-distorted system. As already mentioned, this fact is straightforwardly related to the changes in the dye symmetry, and thus in the absorption spectra. Additionally, the N—OH distance of 1.87 Å found further confirms this assumption. As a consequence of the electronic

Table 2
K_B values for the different calculation alternatives.

	K_B	R
Absorption maxima	$(2.7 \pm 0.2) \times 10^3$	0.999
Absorption areas	$(0.95 \pm 0.05) \times 10^3$	0.996
Quantum yield	$(2.2 \pm 0.2) \times 10^3$	0.999
Fluorescence maxima shift	$(2.8 \pm 0.8) \times 10^3$	0.977

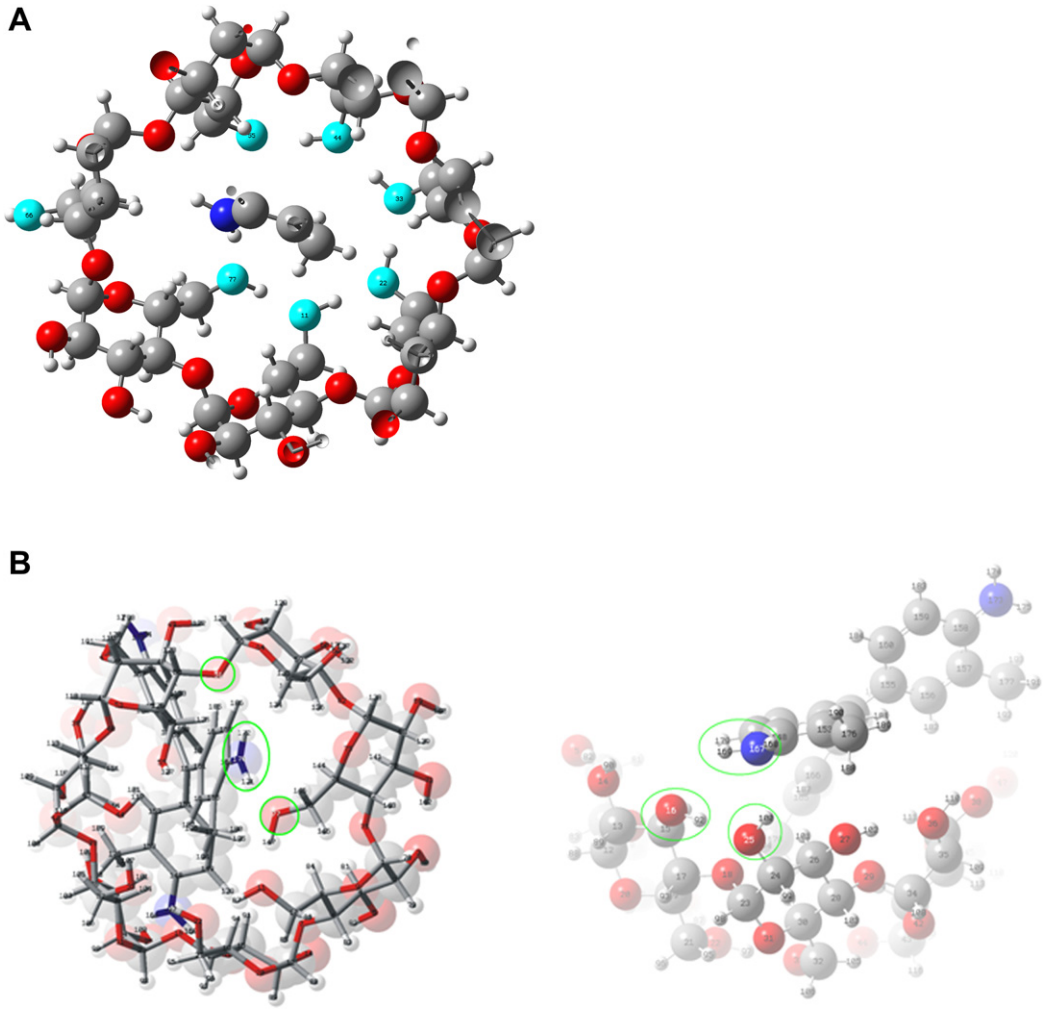

Fig. 6. Tridimensional structure for the NF-β-CD inclusion complex model. A: Cross section view of the complex. Highlighted oxygen atoms belonging to hydroxyl groups. B: View of different arrangements to clarify the main groups involved in the interaction.

delocalization, an increased double bond character in N–C bond is generated.

On the other hand, the nitrogen atom of one of the rings outside the β-CD cavity interacts by hydrogen bond with one of the secondary hydroxyls situated in the upper zone of the cavity. In Table 3, it is possible to see that the delocalization giving rise to the interaction ($Lp(2)\ O_{16} \rightarrow \sigma^{*}C_{149}{-}H_{179}$) occurs in both distorted and not-distorted systems. However, it is stronger in the former (1.09 Kcal mol^{-1}). The resultant complex conformation is achieved when the incoming ring approaches with an angle close to 30° with respect to the normal (Fig. 6B).

Table 3
Delocalization effects, orbital occupancies and stabilization energies for both inclusion complexes.

Orbitals[a]	Occupancy of acceptor orbital		Energies of stabilization (Kcal/mol)	
	Distorted complex	Not-distorted complex	Distorted complex	Not-distorted complex
$Lp(2)\ O_{16} \rightarrow \sigma^{*}C_{149}{-}H_{179}$	0.0161	0.0067	1.09	0.09
$Lp(1)\ O_{51} \rightarrow \sigma^{*}N_{170}{-}H_{172}$	0.0192	–	2.89	–
$Lp(2)\ O_{77} \rightarrow \sigma^{*}N_{170}{-}H_{171}$	0.0482	–	16.93	–
$Lp(1)\ N_{167} \rightarrow \sigma^{*}O_{25}{-}H_{100}$	0.0252	–	5.60	–
$\sigma N_{170}{-}H_{171} \rightarrow \sigma^{*}C_{163}{-}C_{164}$	0.0238	0.0155	3.97	1.94

[a] For atom numbering see Fig. 6B.

4. Conclusion

HP-β-CDs include Basic Violet 2 to form host–guest complex and alter the spectroscopy properties of this dye. The enhancement in fluorescence intensity, the shifts in the maximum of absorption in aqueous solution and the theoretical calculi performed corroborate the inclusion complexes. Experimental and theoretical results were used to evaluate the association constants; the values of association constants determined are in agreement with each other indicating that the stability of the complex depends on the hydrophobicity of the guest molecule; the changes produced in the absorption spectrum can be successfully represented theoretically as composing of only two gaussian functions. The results of the theoretical calculations demonstrated that the formation of the complex modifies the symmetry of the dye since, free in solution, it presents equilibrium between D_3 and C_2 symmetry, displaced to C_2 symmetry when the dye is included in the HP-β-CDs cavity. Gaussian 03 software at the B3LYP/6-31G level together with the NBO analysis were used to perform molecular orbital conformational analysis to support the complex stability.

Acknowledgments

The authors thank Consejo Nacional de Investigaciones Científicas y Técnicas de Argentina (CONICET), Secretaría de Ciencia y Técnica (SECyT), Facultad de Ciencias Químicas de la Universidad Nacional de Córdoba, and Agencia Nacional de Promoción de la Ciencia y Técnica (ANPCYT) for financial support.

References

[1] Morgan J, Oseroff AR. Mitochondria-based photodynamic anti-cancer therapy. Advanced Drug Delivery Reviews 2001;49:71–86.
[2] Mang TS, Sullivan M, Cooper M, Loree T, Rigual N. The use of photodynamic therapy using 630 nm laser light and porfimer sodium for the treatment of oral squamous cell carcinoma. Photodiagnosis and Photodynamic Therapy 2006;3:272–5.
[3] Dougherty TJ. Photosensitizers: therapy and detection of malignant tumors. Photochemistry and Photobiology 1987;45:879–89.
[4] Henderson BW, Dougherty TJ. Photodynamic therapy: basic principles and clinical applications. New York: Marcel Dekker; 1992.
[5] Berlanda J, Kiesslich T, Engelhardt V, Krammer B, Plaetzer K. Comparative in vitro study on the characteristics of different photosensitizers employed in PDT. Journal of Photochemistry and Photobiology B: Biology 2010;100:173–80.
[6] (a) Davis S, Weiss MJ, Wong JR, Lampidis TJ, Chen LB. Mitochondrial and plasma membrane potentials cause unusual accumulation and retention of rhodamine 123 by human breast adenocarcinoma-derived MCF-7 cells. The Journal of Biological Chemistry 1985;260:13844–50;
(b) Indig GL, Lacerda SHD, Abraham B, Stringfellow TC. Photophysical, photochemical, and tumor-selectivity properties of bromine derivatives of rhodamine-123. Photochemistry and Photobiology 2005;81:1430–8.
[7] Kandela IK, Bartlett JA, Indig GL. Effect of molecular structure on the selective phototoxicity of triarylmethane dyes towards tumor cells. Photochemical & Photobiological Sciences 2002;1:309–14.
[8] Fair V, Thomas S, Mathew SC, Abhilash KG. Recent advances in the chemistry of triaryl- and triheteroarylmethanes. Tetrahedron 2006;62:6731–47.
[9] Allison RR, Sibata CH. Oncologic photodynamic therapy photosensitizers: a clinical review. Photodiagnosis and Photodynamic Therapy 2010;7:61–75.
[10] Szejtli J. Introduction and general overview of cyclodextrin chemistry. Chemical Reviews 1998;98:1743–54.
[11] Wainwright M. Photodynamic antimicrobial chemotherapy (PACT). Journal of Antimicrobial Chemotherapy 1998;42:13–28.
[12] Araújo Prates R, Massayoshi Yamada Jr A, Suzuki LC, Eiko Hashimoto MC, Cai S, Gouw-Soares S, et al. Bactericidal effect of malachite green and red laser on Actinobacillus Actinomycetemcomitans. Journal of Photochemistry and Photobiology B: Biology 2007;86:70–6.
[13] Mauricio S, Baptista MS, Indig GL. Effect of BSA binding on photophysical and photochemical properties of triarylmethane dyes. Journal of Physical Chemistry B 1998;102:4678–88.
[14] Bhasikuttan AC, Sapre AV, Shastri LV. Photoinduced electron transfer in crystal violet (CV^+)–bovine serum albumin (BSA) system: evaluation of reaction paths and radical intermediates. Journal of Photochemistry and Photobiology A: Chemistry 2002;150:59–66.
[15] Santhanalakshmi J, Balaji S. Binding studies of crystal violet on proteins. Colloids and Surfaces A: Physicochemical and Engineering Aspects 2001;186:173–7.
[16] Korppi-Tommola J, Yip RW. Solvent effects on the visible absorption spectrum of crystal violet. Canadian Journal of Chemistry 1981;59:191–4.
[17] Lewis LM, Indig GL. Solvent effects on the spectroscopic properties of triarylmethane dyes. Dyes and Pigments 2000;46:145–54.
[18] Wolfe AD. Influence of cationic triphenylmethane dyes upon DNA polymerization and product hydrolysis by *Escherichia coli* polymerase I. Biochemistry 1977;16(1):30–3.
[19] Preat J, Jacquemin D, Wathelet V, André JM, Perpète EA. Towards the understanding of the chromatic behaviour of triphenylmethane derivatives. Chemical Physics 2007;335:177–86.
[20] Kowaltowski AJ, Turin J, Indig GL, Vercesi AE. Mitochondrial effects of triarylmethane dyes. Journal of Bioenergetics and Biomembranes 1999;31(6):581–90.
[21] Lewis GN, Magel YT, Lipkin D. Isomers of crystal violet ion. Their absorption and re-emission of light. Journal of the American Chemical Society 1942;64:1774–82.
[22] Sundstöm V, Gillbro T. Effects of solvent on TMP photophysics. Transition from no barrier to barrier case, induced by solvent properties. Journal of Chemical Physics 1984;81:3463–75.
[23] Clark FT, Drickamer HG. The effect of pressure on the adsorption of crystal violet on oriented ZnO crystals. Journal of Chemical Physics 1984;81:1024–9.
[24] Clark FT, Drickamer HG. High-pressure study of triphenylmethane dyes in polymeric and aqueous media. Journal of Physical Chemistry 1986;90(4):589–92.
[25] Maruyama Y, Ishikawa M, Satozono H. Femtosecond isomerization of crystal violet in alcohols. Journal of the American Chemical Society 1996;118:6257–63.
[26] Gomez de Mesquita AH, MacGillvry CH, EriKs K. The structure of triphenylmethyl perchlorate at 85 °C. Acta Crystallographica 1965;18(3):437–43.
[27] Dekkers HPJM, Kielman-Van Luyt ECM. Magnetic circular dichroism of the triphenylcarbenium ion and some symmetrically para-substituted derivatives. Molecular Physics 1976;31(4):1001–19.
[28] Angeloni L, Smulevich G, Marzocchi MP. Resonance Raman spectrum of crystal violet. Journal of Raman Spectroscopy 1979;8(6):305–10.
[29] Korppi-Tommola J, Yip RW. Solvent effects on the visible absorption spectrum of crystal violet. Canadian Journal of Chemistry 1981;59(2):191–4.
[30] Lueck HB, McHale JL, Edwards WD. Symmetry-breaking solvent effects on the electronic structure and spectra of a series of triphenylmethane dyes. Journal of the American Chemical Society 1992;114(7):2342–8.
[31] Bernard Bernard MJ, García-Mora J, Díaz D, Mendoza Díaz G. Molecular interactions and thermodynamic aspects of the complexation reaction between Gentian violet and several cyclodextrins. Journal of Inclusion Phenomena and Macrocyclic Chemistry 1999;34(1):1–18.
[32] García–Río L, Godoy A, Leis JR. Spectroscopic characterisation of crystal violet inclusion complexes in β-cyclodextrin. Chemical Physics Letters 2005;401:302–6.
[33] Montes de Oca MN, Aiassa I, Argüello G, Ortiz C. Separation, purification, and characterization of analogues components of a commercial sample of New Fuchsin. Journal of Chromatographic Science 2010;48:618–23.
[34] Benesi H, Hildebrand J. A spectrophotometric investigation of the interaction of iodine with aromatic hydrocarbons. Journal of the American Chemical Society 1949;71(8):2703–7.
[35] Gaspar de Araujo MV, Macedo OFL, Da Cunha Nascimento C, Conegero LS, Barreto LS, Almeida LE, et al. Characterization, phase solubility and molecular modeling of α-cyclodextrin/pyrimethamine inclusion complex. Spectrochimica Acta Part A 2009;72:165–70.
[36] Gaspar de Araujo MV, Barbosa Vieira EK, Lázaro GS, Conegero LS, Ferreira OP, Almeida LE, et al. Inclusion complexes of pyrimethamine in 2-hydroxypropyl-β-cyclodextrin: characterization, phase solubility and molecular modeling. Bioorganic & Medicinal Chemistry 2007;15:5752–9.
[37] Lee C, Yang W, Parr RG. Development of the Colle-Salvetti correlation-energy formula into a functional of the electron density. Physical Review B 1988;37(2):785–9.
[38] Becke AD. Density functional thermochemistry. III. The role of exact exchange. Journal of Chemical Physics 1993;98(7):5648–53.
[39] Becke AD. A new mixing of Hartree–Fock and local density-functional theories. Journal of Chemical Physics 1993;98(2):1372–8.
[40] Frisch MJ, Trucks GW, Schlegel HB, Scuseria GE, Robb MA, Cheeseman JR, et al. Gaussian 03, Revision B.04. Pittsburgh PA: Gaussian, Inc.; 2003.
[41] Brunck TK, Weinhold F. Quantum-mechanical studies on the origin of barriers to internal rotation about single bonds. Journal of the American Chemical Society 1979;101(7):1700–9.
[42] E.D. Glendening, A.E. Reed, J.E. Carpenter, F. Weinhold, NBO version 3.1.
[43] Feliciano CE, Quiñones E. The association of 4-(*N*, *N*-dimethylamino)benzonitrile and β-cyclodextrin in dimethyl sulfoxide and *N*, *N*-dimethylformamide. Journal of Photochemistry and Photobiology A: Chemistry 1999;120(1):23–8.
[44] Zhang G, Shuang S, Dong Z, Dong C, Pan J. Investigation on the inclusion behavior of neutral red with β-cyclodextrin, hydroxypropyl- β -cyclodextrin and sulfobutylether- β –cyclodextrin. Analytica Chimica Acta 2002;474:189–95.
[45] Zhu X, Sun J, Wu J. Study on the inclusion interactions of β-cyclodextrin and its derivative with dyes by spectrofluorimetry and its analytical application. Talanta 2007;72(1):237–42.
[46] Oliveira CS, Branco KP, Baptista MS, Indig GL. Solvent and concentration effects on the visible spectra of tri-para-dialkylamino-substituted triarylmethane dyes in liquid solutions. Spectrochimica Acta Part A: Molecular and Biomolecular Spectroscopy 2002;58(13):2971–82.
[47] García-Río L, Godoy A. Influence of CTACl cationic micelles on the spectral behavior of crystal violet. Chemical Physics 2006;327:361–7.
[48] García-Río L, Hervella P, Mejuto JC, Parajó M. Spectroscopic and kinetic investigation of the interaction between crystal violet and sodium dodecylsulfate. Chemical Physics 2007;335:164–76.
[49] Tafazzoli M, Ghiasi M. Structure and conformation of α-, β- and γ-cyclodextrin in solution: theoretical approaches and experimental validation. Carbohydrate Polymers 2009;78(1):10–5.